The Impacts of the 9 April 2009 Dust and Smoke on Convection

BY DANIEL T. LINDSEY, STEVEN D. MILLER, AND LOUIE GRASSO

Wildfires and dust storms, although less frequent than severe thunderstorms, are not uncommon to the United States, and in some cases can have disastrous impacts to life and property. In the central plains, wildfires and dust storms occur in concert with very strong, dry winds, often behind a surface dryline associated with a powerful midlatitude cyclone. Strong synoptic systems often generate severe convection within their warm sectors. This is also a preferred location for wildfire and dust outbreaks, provided favorable surface conditions exist in terms of dry vegetation and erodible surfaces, respectively. The proximity of warm-sector convection to boundary layer smoke and dust, when present, leads to the possibility of these aerosols mixing into the storms at the low- and midlevels and potentially altering the microphysical development of these cloud systems. Presented here are satellite observations of both the aerosols and the anomalous cloud-top microphysical evolution observed for a case of convection over the Great Plains, which provide further evidence to a growing body of scientific research suggesting the two are closely linked.

Little is presently known about what effects such combined (dust and smoke) aerosol ingestion has on convection. In a 2004 article in *Science,* Andreae et al. discuss how convective clouds forming near wildfires in the Amazon have reduced cloud droplet sizes due to the increased influx of cloud condensation nuclei (CCN) by dust and smoke aerosols to the relatively pristine environment. They argue that smaller droplets decrease the collision-coalescence efficiency, which effectively delays the evolution of precipitation-sized droplets and shifts the water mass upward in the cloud. They also argue that shifting the precipitation production upward results in more vigorous updrafts and stronger storms.

Other work related to the impacts of aerosols on deep convection include Lindsey and Fromm (2008), who observed pyrocumulonimbus (pyroCb) clouds, or storms initiated by the intense heat of a wildfire. Using Geostationary Operational Environmental Satellite (GOES) imagery, they found that pyroCbs exhibited unusually small cloud-top ice crystals as determined from multispectral observations, which the researchers attributed to ingestion of wildfire-produced biomass aerosols. Convective clouds that were displaced from the wildfire aerosol source (but in an environment with the same general stability characteristics) displayed significantly larger cloud-top particle sizes. They hypothesized that the smoke served as a source of enhanced CCN, and like the Amazonian clouds discussed above, an unusually large number of cloud droplets nucleated near cloud base. These droplets were then lofted within the vigorous updrafts of the storm, where they froze homogeneously above the −40°C level and populated the storms' anvils with tiny ice crystals (see the conceptual diagram in Fig. 1). The anvils of these pyroCbs persisted for longer than those of the regular convection, a good example of the cloud lifetime effect. Presumably, smaller cloud droplets decreased the precipitation efficiency of the storm, and more water mass was lofted to the anvil, where it resided longer before either sublimating or falling out. This process is also considered an aerosol indirect effect, where aerosols alter cloud properties (such as the lifetime of the cloud), which in turn affect incoming and/or outgoing radiation. In a 2005 article in the *Journal of the Atmospheric Sciences,* Heymsfield et al. propose an alternative mechanism that involves aerosol particles being entrained into convection at

AFFILIATIONS: LINDSEY—NOAA/NESDIS/STAR/RAMMB, Fort Collins, Colorado; MILLER AND GRASSO—Cooperative Institute for Research in the Atmosphere, Fort Collins, Colorado
CORRESPONDING AUTHOR: Daniel T. Lindsey, CIRA/Colorado State University, 1375 Campus Delivery, Ft. Collins, CO 80523-1375
E-mail: Dan.Lindsey@noaa.gov

DOI: 10.1175/2010BAMS2964.1

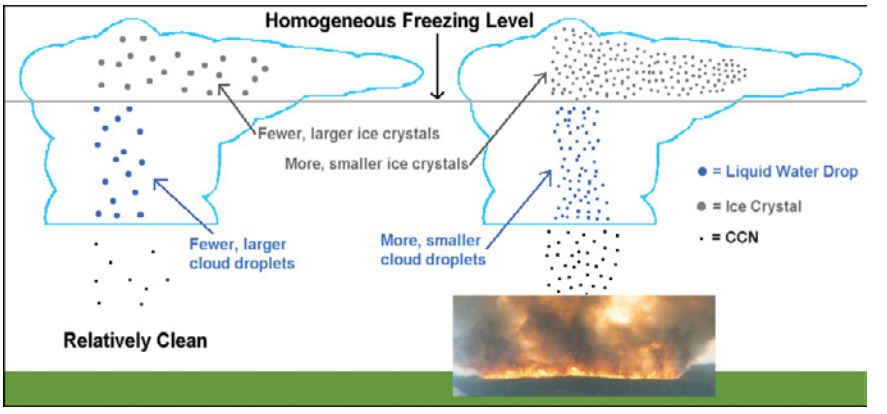

Fig. 1. Conceptual diagram comparing (left) a relatively pristine environment to (right) a polluted environment (such as downwind of a fire, as represented by the photo). The number of CCN and the size and number of ice crystals and liquid water drops are qualitatively represented by the number and size of black, gray, and blue dots, respectively. In a more polluted environment, the additional CCN result in more and smaller cloud droplets, which are lofted above the homogeneous freezing level where they freeze to produce a larger number of smaller ice crystals. Other hydrometeors (such as midlevel ice and precipitation-sized particles) are not represented in this diagram.

midlevels, activating droplets there, then freezing homogeneously and producing small anvil ice crystals. Both mechanisms are consistent with the idea that increased aerosol concentrations can lead to smaller ice crystals at the tops of deep convection.

The impact of fire and dust aerosols on convection is examined here using GOES imagery for a convective event that occurred over the central United States on 9 April 2009. On this day, environmental conditions favorable for strong warm-sector convection set up across Texas and Oklahoma. In addition, strong winds near the dryline generated a large dust storm and a number of fast-moving grassland fires in the immediate vicinity of the convection. In their 2010 *BAMS* article, Jones and Christopher provide details on the observation of the dust, fires, and smoke from this case, as well as some of the damage associated with the fires. Convection later initiated along the surging dryline, and smoke and dust aerosols were observed feeding into the rear flank of the thunderstorms.

To introduce this case study from the satellite perspective, Fig. 2a shows a MODIS image from 9 April 2009 at 1930 UTC from the NexSat Web site (www.nrlmry.navy.mil/NEXSAT.html), enhanced for mineral dust via the multispectral technique outlined by Miller (2003). Dust appears as red tones in this enhancement, and can be seen across much of north Texas. Also labeled on this image are smoke plumes from a number of fires along the eastern end of the dust. The north-south line of clouds in east Texas and Oklahoma denotes the location of the dryline, and convection is just beginning to initiate on its northern end at the time of the satellite overpass. The dust enhancement in Fig. 2a shades only the pixels with the highest dust concentrations red (e.g., visible optical depths greater than about 0.5), but lower concentrations may exist in proximity to these red pixels. For example, gusty winds were observed in central Oklahoma behind the dryline, so widespread dust was likely to be present there.

By 2145 UTC, storms in eastern Oklahoma had matured, and a solid bank of smoke and/or dust can be seen adjacent to the western edge of the convective line (Fig. 2b). The proximity of the significant aerosol species to the active convection suggests that some must be mixing with the clouds either at low- or midlevels. As shown by Jones and Christopher (2010), grassfire debris in this event was detected by radar up to 5 km AGL, so the smaller aerosols were very likely lofted to at least this height.

GOES imagery provides high temporal resolution so that convective evolution can be easily monitored. It also features a shortwave infrared channel at 3.9 μm that is of particular utility to this analysis. The amount of solar 3.9-μm radiation reflected by deep convective clouds is strongly dependent on the size of ice crystals populating the uppermost portions of the anvil. This dependence allows one to retrieve the ice effective radius[1] at cloud-top, and when combined with the frequency of GOES scans, one can examine the trends in cloud-top microphysical structure.

[1] Effective radius is defined here as

$$r_e = \frac{3}{4}\frac{\int_{D_{MIN}}^{D_{MAX}} V(D)N(D)dD}{\int_{D_{MIN}}^{D_{MAX}} A(D)N(D)dD},$$

where $V(D)$ is the ice crystal volume and $A(D)$ is the crystal projected area. $N(D)$ is the ice crystal number.

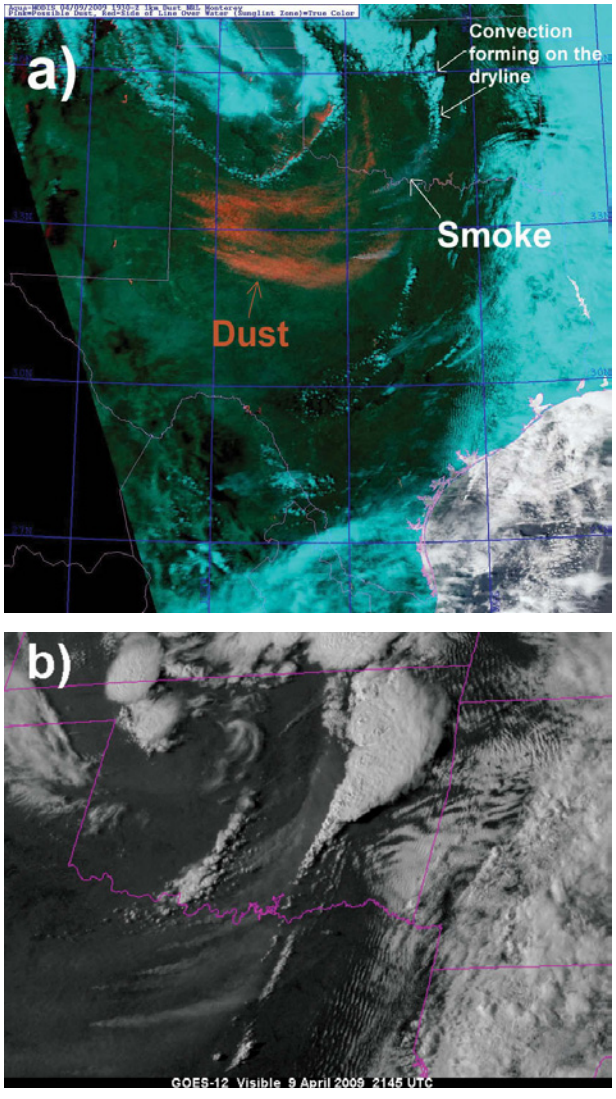

Fig. 2. (a) Aqua-MODIS image from 9 Apr 2009 at 1930 UTC, enhanced to highlight areas of dust. Multiple point sources of dust are present in the Texas panhandle, and behind a developing convective line extending into western Oklahoma. Smoke plumes to the east of the main dust areas appear as gray, and meteorological clouds are shown in cyan. Imagery provided by the Naval Research Laboratory NexSat project (www.nrlmry.navy.mil/NEXSAT.html). (b) Visible satellite image from *GOES-12* at 2145 UTC on 9 Apr 2009. Dust, smoke, and vigorous convection are all evident across Oklahoma and Texas.

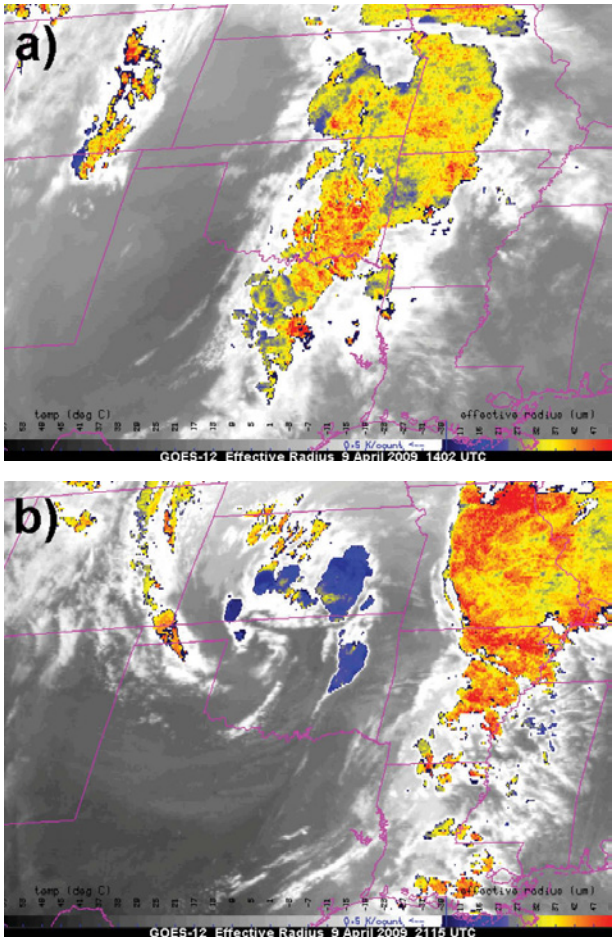

Fig. 3. Retrieval of ice effective radius (μm) for clouds with 10.7-μm brightness temperatures less than −40°C (colors), and 10.7-μm brightness temperature for pixels warmer than −40°C (grayscale) based on *GOES-12* imagery at (a) 1402 UTC and (b) 2115 UTC on 9 Apr 2009.

Details on how this retrieval is formulated can be found in Lindsey and Grasso's 2008 *Journal of Applied Meteorology and Climatology* article.

The retrieved cloud-top effective radius on 9 April at two times on is shown in Fig. 3. At 1402 UTC, before large aerosol concentrations were present, weak morning convection was moving out of Texas and Oklahoma; ice effective radius values of these clouds generally ranged from 35 to 45 μm. By 2115 UTC (Fig. 3b), those storms had moved into eastern Arkansas and Missouri, and new convection was forming along the dryline in eastern Oklahoma and northeast of the surface low in southern Kansas. Ice effective radius values of the storms in this turbid environment were generally less than 20 μm (the blue colors in Fig. 3b), with a few storms generating ice crystals with effective radii as low as 10 μm. New storms formed along the dryline in east Texas after 2300 UTC, but the sun angle was too steep at these hours to allow for a reliable ice effective radius retrieval.

A single case study provides no information about climatological mean values. However, climatology

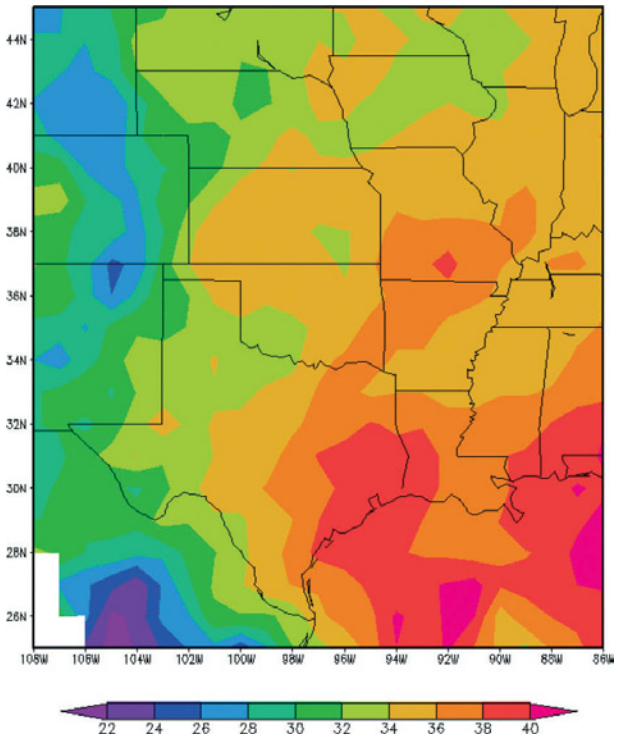

Fig. 4. Mean ice cloud effective radius (μm) for all pixels having 10.7-μm brightness temperatures colder than −40°C, based on data from Mar 2000, 2003, 2004, and Apr 2000, 2004.

can be used to examine differences between the 9 April event and events not contaminated with aerosols. For this purpose, we used three years of data (March 2000, 2003, 2004, and April 2000, 2004; periods offering contiguous data) to generate a map of mean ice crystal effective radius (Fig. 4). The months of March and April were selected to remove any interseasonal variations. To calculate the mean, the ice effective radius was retrieved for all pixels whose 10.7-μm brightness temperature was less than −40°C, which included both convective and nonconvective thick cirrus clouds. However, a visual inspection of the older data reveals that the grand majority of the thick cirrus over the southern plains was convectively generated. Mean ice crystal effective radius values are 34–40 μm across Texas and Oklahoma, with standard deviations around 8 μm (not shown). Comparing this map to the retrieval shown in Fig. 3b, the cloud tops on 9 April showed ice effective radius values generally 1–2 standard deviations below the mean. Histograms comparing the ice effective radii from the afternoon convection on 9 April to those of climatology (Fig. 5) also show that the convectively generated ice crystals on 9 April were smaller than is typical.

In the absence of in situ data, a causal relationship between the presence of significant aerosol concentrations and the anomalous cloud top microphysics observed from satellite can only be postulated. Unanswered questions include:

1) What other cloud processes alter cloud-top ice crystal size?
2) What effects do different species of aerosol have on the intensity of the convection?
3) Do the smaller cloud-top ice crystals significantly alter the radiation budget?

Ongoing research is addressing these important questions, but to fully understand how aerosols affect clouds and the full spectrum of potential feedbacks, additional collaboration is needed among cloud physicists, modelers, chemists, satellite meteorologists, and theoretical radiative transfer experts. In terms of remote-sensing capabilities, the next generation of geostationary satellites, GOES-R, is scheduled to be launched in 2015. The Advanced Baseline Imager aboard GOES-R will provide improved spectral, spatial, and temporal resolution, and will significantly improve our ability to study the microphysical aspects of thunderstorms.

ACKNOWLEDGMENTS. This material is based on work supported by the National Oceanic and Atmospheric Administration under Grant NA090AR4320074. The

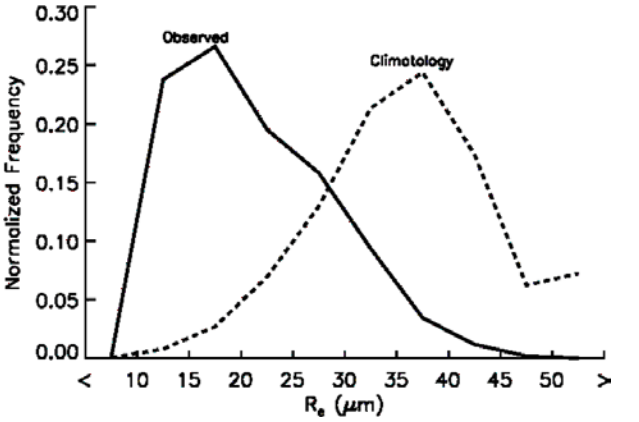

Fig. 5. Histograms showing the normalized frequency of ice effective radius for the 9 Apr 2009 event over the southern plains (solid), and for the climatology using the same data as in Fig. 4 (dashed). For both histograms, only data north of 29°N, south of 40°N, east of 100°W, and west of 95°W were used. Effective radius is defined here as in the footnote on page 992.

authors would like to thank John Knaff, Don Hillger, and Mark DeMaria for providing useful critical reviews, as well as three anonymous reviewers for useful comments. The views, opinions, and findings in this report are those of the authors, and should not be construed as an official NOAA and/or U.S. Government position, policy, or decision.

FOR FURTHER READING

Andreae, M. O., D. Rosenfeld, P. Artaxo, A. A. Costa, G. P. Frank, K. M. Longo, and M. A. F. Silvas-Dias, 2004: Smoking rain clouds over the Amazon. *Science,* **303,** 1337–1342.

Heymsfield, A. J., L. M. Miloshevich, C. Schmitt, A. Bansemer, C. Twohy, M. R. Poellot, A. Fridlind, and H. Gerber, 2005: Homogeneous ice nucleation in subtropical and tropical convection and its influence on cirrus anvil microphysics. *J. Atmos. Sci.,* **62,** 41–64.

Jones, T. A., and S. A. Christopher, 2010: Satellite and radar observations of the 9 April 2009 Texas and Oklahoma grassfires. *Bull. Amer. Meteor. Soc.,* **91,** 455–460, doi:10.1175/2009BAMS2919.1.

Lindsey, D. T., and M. Fromm, 2008: Evidence of the cloud lifetime effect from wildfire-induced thunderstorms. *Geophys. Res. Lett.,* **35,** L22809, doi:10.1029/2008GL035680.

——, and L. Grasso, 2008. An effective radius retrieval for thick ice clouds using GOES. *J. Appl. Meteor. Climatol.,* **47,** 1222–1231.

Miller, S. D., 2003: A consolidated technique for enhancing desert dust storms with MODIS. *Geophys. Res. Lett.,* **30,** 2071–2074.

——, and Coauthors, 2006: NexSat: Previewing NPOESS/VIIRS imagery capabilities. *Bull. Amer. Meteor. Soc.,* **87,** 433–446, doi:10.1175/BAMS-87-4-433.

Schmit, T. J., M. M. Gunshor, W. P. Menzel, J. J. Gurka, J. Li, and A. S. Bachmeier, 2005: Introducing the next-generation advanced baseline imager on GOES-R. *Bull. Amer. Meteor. Soc.,* **86,** 1079–1096.

Radar and Atmospheric Science: A Collection of Essays in Honor of David Atlas

Edited by Roger M. Wakimoto and Ramesh Srivastava

This monograph pays tribute to one of the leading scientists in meteorology, Dr. David Atlas. In addition to profiling the life and work of the acknowledged "Father of Radar Meteorology," this collection highlights many of the unique contributions he made to the understanding of the forcing and organization of convective systems, observation and modeling of atmospheric turbulence and waves, and cloud microphysical properties, among many other topics. It is hoped that this text will inspire the next generation of radar meteorologists, provide an excellent resource for scientists and educators, and serve as a historical record of the gathering of scholarly contributions honoring one of the most important meteorologists of our time.

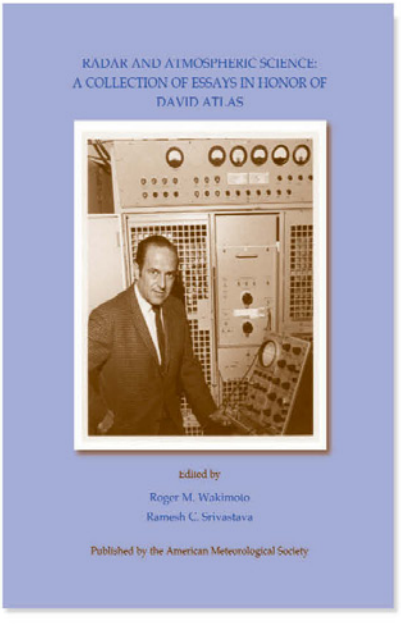

Radar and Atmospheric Science: A Collection of Essays in Honor of David Atlas

Aug 2003. Meteorological Monograph Series, Vol. 30, No. 52; 270 pp, hardbound; ISBN 1-878220-57-8; AMS code MM52.

Price $100.00 list/$80.00 member

To place an order submit your prepaid orders to AMS, Attn: Order Dept, 45 Beacon St. Boston, MA 02108-3693

Order by phone using Visa, Mastercard, or American Express (617) 227-2426 x. 686 or **E-mail** amsorder@ametsoc.org

Please make checks payable to the *American Meteorological Society*.